Supporting Information

Zhang et al. 10.1073/pnas.1108052108

SI Materials and Methods

DNA Constructs. The cDNA for human and murine T-cell receptor ζ (TCRζ) was obtained commercially (Geneservice Ltd). Mutations, truncations, and extracellular chimeric constructs were generated by PCR-based mutagenesis strategies and confirmed by dsDNA sequencing (Source BioScience). The extracellular domain of rat CD2 (amino acids 1–202) was used in the chimeric constructs with a linker serine, threonine, and then the transmembrane and cytosolic domain of TCRζ (amino acids 31–165) followed by a linker of proline, arginines, arginines, threonine, and then the fluorescent protein. The protein sequence of TCRζ and the location of the defined immunoreceptor tyrosine-based activation motifs (ITAMs), basic rich stretch (BRS) motifs, and the transmembrane and extracellular domains are illustrated in Fig. S1. Mutations of the ITAMs were generated by mutating TCRζ ITAM tyrosines to phenylalanine. Mutations of the BRS motifs were generated by mutating all the arginines and lysines in the BRS motifs to alanine. All constructs were tagged at the C terminus with either teal fluorescent protein (TFP) (a gift from Daniel Choquet, Centre National de la Recherche Scientifique, Bordeaux, France) or DsRed (Clontech). The various TCRζ-modified constructs were cloned into the vectors pHR-SIN-BX-IRES-Em or pBMN, which were obtained from the Nolan laboratory (Stanford University, Stanford, CA). GST-fusion proteins were generated using pGEX-2TK vectors (GE Biosciences) and purified with MagneGST Protein Purification System (Promega).

TCRζ Mobility Measurements by Fluorescence Recovery After Photobleaching. B3Z T cells with BRS intact or mutated containing TFP at the TCRζ cytoplasmic tail were loaded into an imaging chamber (Attofluor cell chamber, A-7816; Invitrogen) with Tyrode buffer. Imaging was focused at the periphery of the plasma membrane, and the optical section in the confocal was 1.1 μm for the 458-nm laser. During the bleaching phase, a 1.3 ×1.3 μm region of interest (ROI) at the very edge of the cell membrane was bleached at 458 nm in full laser power for five cycles. Then a series of time-lapse images was taken with the same laser (3% power). Next, the average intensity of ROI in each image was measured and plotted. We fit an exponential model to the fluorescence recovery data to obtain estimates of the mobile fraction (M_f) and the timescale of fluorescence recovery (τ),

$$I = \left(1 - \frac{F_0}{F_P}\right) M_f(1 - \exp(-t / \tau)) + \frac{F_0}{F_P} \quad [1]$$

where F_P and F_0 are the pre- and postbleaching fluorescence intensity, respectively. Data fitting was performed as previously described (1), using the MATLAB (The MathWorks, Natick, MA) function lsqcurvefit, which provides estimates of M_f and τ.

In Vitro Lymphocyte Cell-Specific *Protein*-Tyrosine Kinase Assay. GST-fusion proteins of only the cytoplasmic domains of TCRζITAM2, TCRζITAM2 without the BRS motif (B–) and TCRζ without ITAM2 (I–) were generated (Fig. 1*A*) using pGEX-2TK vectors (GE Biosciences) and purified with the MagneGST Protein Purification System (Promega) from Rosetta BL21 (DE3) pLysS e-coil (Novagen). Proteins were incubated for 5 min at 37 °C with or without 34 uM lymphocyte cell-specific *protein*-tyrosine kinase (Lck) (Millipore), and the products were analyzed by Western blotting using anti-GST antibody to measure total protein and anti-pY antibody (1G4) for phosphorylated TCRζ. The substrate concentration ranged from 1.3 μM to 325 nM. The location of substrates on SDS protein gels depended on overall size and charge. Nonsaturation of the kinase assay was confirmed by observing a further increase in substrate phosphorylation at an extended time point.

1. Dushek O, Coombs D (2008) Improving parameter estimation for cell surface FRAP data. *J Biochem Biophys Methods* 70:1224–1231.

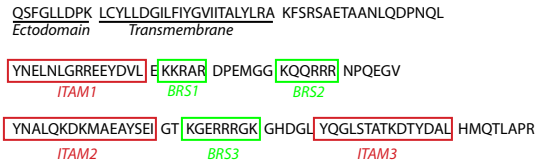

Fig. S1. Amino acid sequence of mouse TCRζ with notation of different domains and motifs. ITAMs are highlighted in red boxes. ITAM-deficient (I–) mutants were generated by the mutation of all tyrosine residues within the red boxes to phenylalanine. BRS motifs (defined here as clusters of three or more consecutive arginine or lysine residues) are highlighted in green boxes. BRS-deficient (B–) mutants were generated by the mutation of all lysine and arginine residues within the green boxes to alanine.

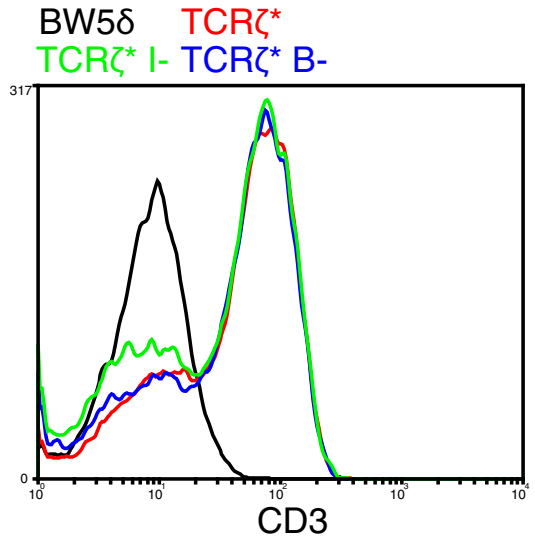

Fig. S2. The expression levels of CD3ε in BW5δ cells before (black line) and after retroviral transduction of the indicated TCRζ constructs as determined by flow cytometry. Cells were surface stained on ice with biotinylated anti-CD3 (145-2C11), washed, and further stained with streptavidin-allophycocyanin before being analyzed by flow cytometry.

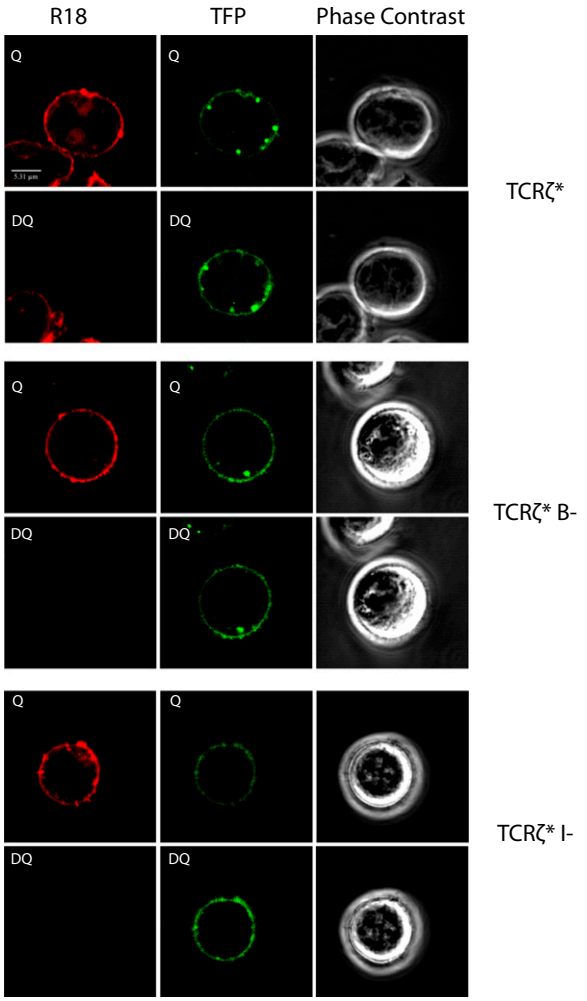

Fig. S3. Association of theTCRζ cytoplasmic domain with the plasma membrane: dependence on BRS motifs. Association was measured by FRET donor dequenching. Constructs used include TCRζ fused to C-terminal TFP (TCRζ*), and two mutant forms of TCRζ* lacking either BRS motifs (TCRζ*B-) or ITAMs (TCRζ*I-). Octadecyl rhodamine B chloride (R18; acceptor) was bleached by a 543-nm laser (full power) for 60–80 s. Panels labeled "Q" show fluorescent images before R18 bleaching (donor quenching); panels labeled "DQ" show fluorescent images after R18 bleaching (donor dequenching).

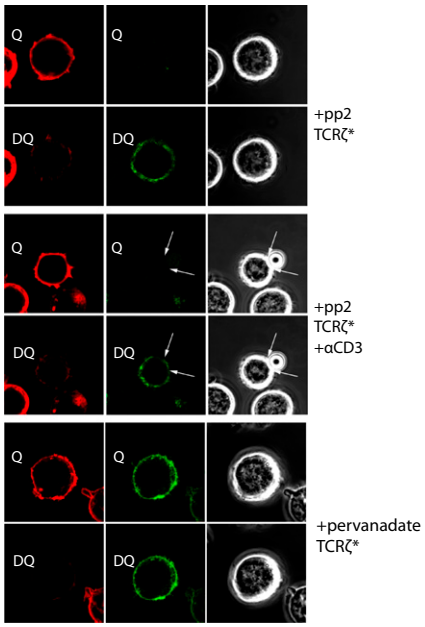

Fig. S4. Dissociation of the TCRζ cytoplasmic domain from the plasma membrane depends on tyrosine phosphorylation. TCRζ*-expressing cells were treated with pervanadate (10 μM) or with PP2 (100 μM), with or without anti-CD3 beads. White arrows show the boundaries of the contact interface between a T cell and an anti-CD3–coated bead. A representative set of images is shown. Quantification is shown in Fig. 1*A*.

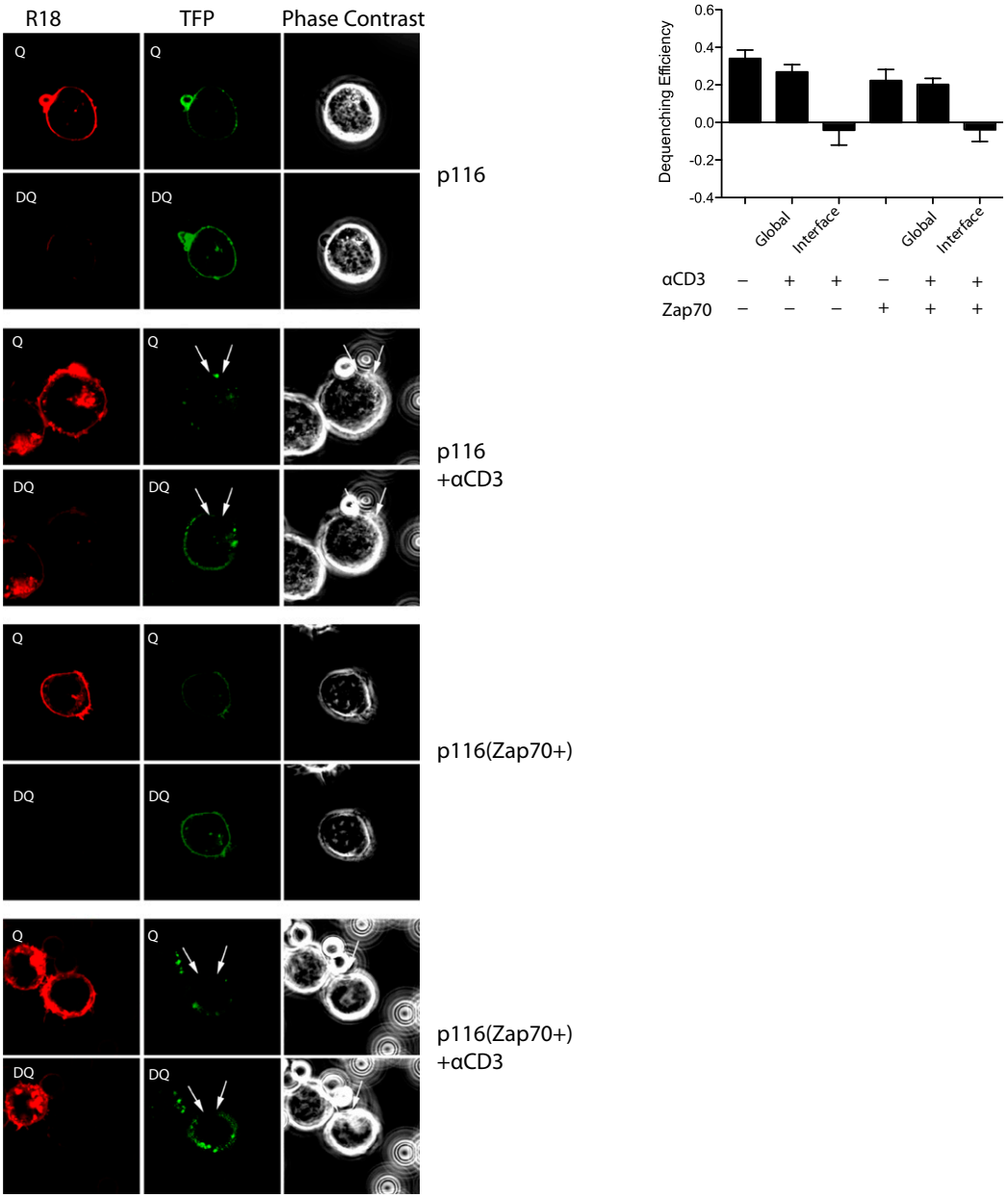

Fig. S5. Dissociation of the cytoplasmic tail of TCRζ from the plasma membrane does not require Zap70 binding. FRET efficiency measurements of Jurkat cells deficient in Zap70 (p116)–expressing human TCRζ*. A proportion of these p116 cells were reconstituted with Zap70 (Zap70+). FRET efficiency with R18 was measured by donor dequenching as described in Fig. 1. Representative images are shown in *A*, and the combined results of multiple (n = 30) images are shown in *B*. In cells stimulated with anti-CD3–coated beads the dequenching efficiency within the bead/cell interface (interface) and outside the interface (global) is shown.

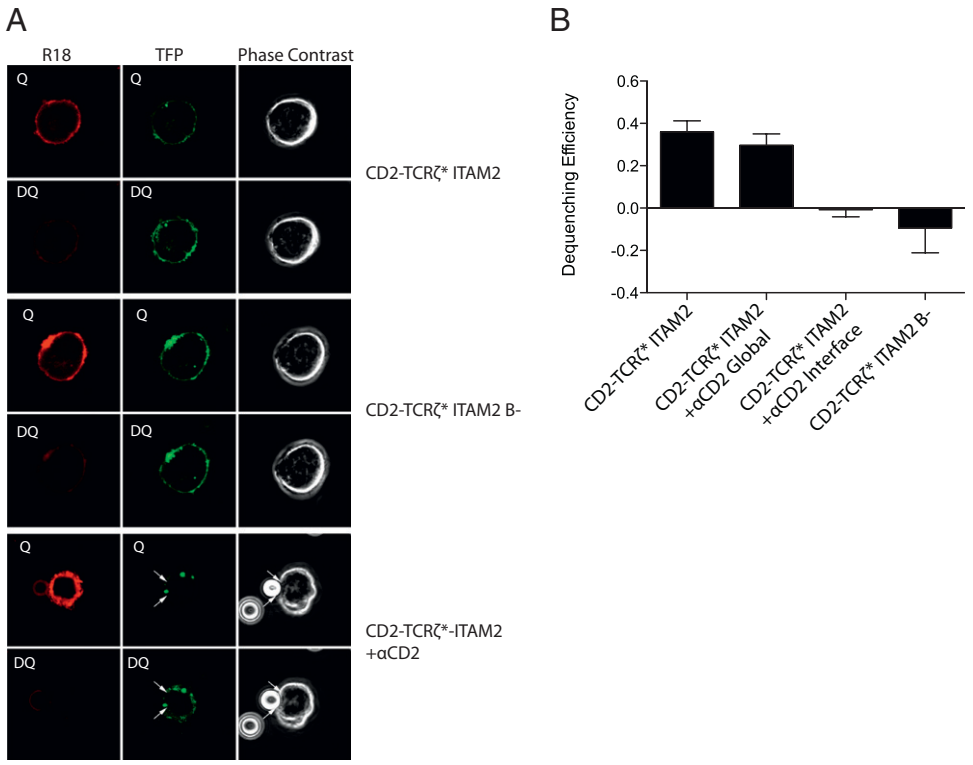

Fig. S6. Association of the cytoplasmic domain of CD2-TCRζ*ITAM2 with the plasma membrane requires BRS motifs and is reversed by ligand engagement. (*A*) Representative images of FRET in BW5δ cells expressing CD2-TCRζ*ITAM2 with or without (B−) the BRS motifs. FRET was measured by donor dequenching as described in Fig. 1. Also shown is dequenching when CD2-TCRζ*ITAM2–expressing cells are stimulate with anti-CD2–coated beads. White arrows denote the boundary of contact areas between a T cell and an anti-CD3–coated bead. (*B*) Quantitation of multiple images (n = 30). In cells stimulated with beads the dequenching efficiency within the bead–cell interface (interface) and outside the interface (global) is shown.

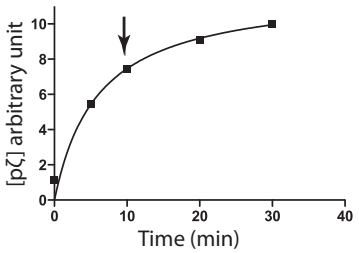

Fig. S7. Phosphorylation of GST-tagged TCRζITAM2 by Lck. In an in vitro kinase assay 325 nM of GST-TCRζITAM2 was incubated with 34 nM of Lck at 37 °C. The reaction was stopped at the indicated times, and products were analyzed by Western blotting with the anti-pY antibody 4G10. The arrow indicates the time point used in Fig. S8. Because the assay is not saturated or at equilibrium under these conditions, a reduction in Lck activity would be detected.

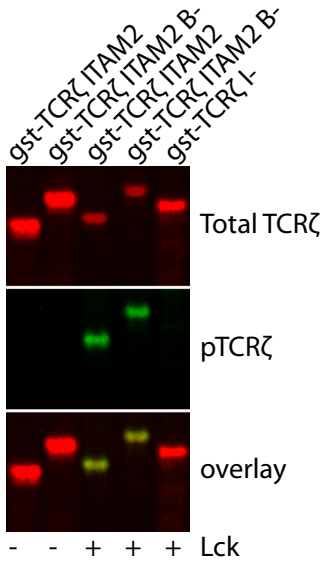

Fig. S8. Mutation of BRS does not affect in vitro phosphorylation of TCRζ by Lck. The indicated proteins were incubated alone or with Lck for 5 min at 37 °C, and the products were analyzed by Western blotting using anti-GST antibody to measure total protein and anti-pY antibody (1G4) for pTCRζ. Control lanes 1, 2, and 5 contained 1.3 μM of substrate, and lanes 3 and 4 contained 325 nM of substrate.

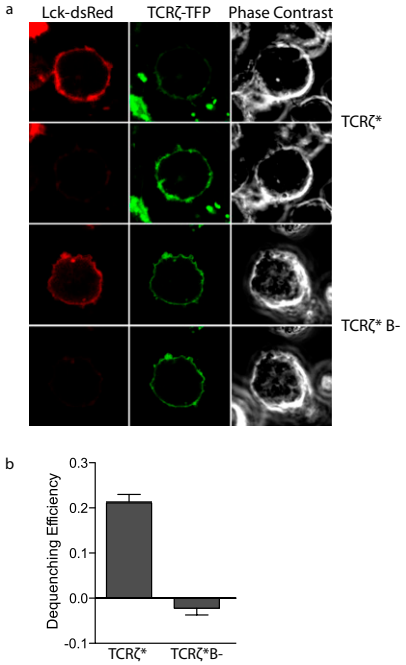

Fig. S9. Association of Lck and TCRζ depends on BRS motifs. (*A*) FRET efficiency measurements using the donor-quenching method on BW5δ cells expressing Lck-DsRed and either TCRζ* or BRS (TCRζ*B–) mutants. Lck-DsRed is the acceptor; TCRζ-TFP is the donor. (*B*) Quantification of the mean dequenching efficiency (E) between Lck-DsRed (acceptor) and TCRζ-TFP (donor) in multiple cells (n = 30). E = (DQ − Q)/DQ.